Investigation of stimulated four-photon parametric scattering of laser radiation in alkali-metal vapor

A. M. Bonch-Bruevich, S. G. Przhibelskiĭ, V. A. Khodovoĭ, and V. V. Khromov

(Submitted January 24, 1973)
Zh. Eksp. Teor. Fiz. **65**, 61–73 (July 1973)

Stimulated four-photon parametric scattering (SFPS) of laser radiation in potassium and rubidium atomic vapor is investigated experimentally and theoretically. SFPS is observed if the wavelength of the exciting light is smaller than the wavelength of the atomic absorption lines and occurs at a single wavelength (degenerate SFPS). The sharp asymmetry of SFPS observed at the long- and short-wave sides of the atomic absorption lines can be explained qualitatively (and in some cases quantitatively) if the attenuation of the strong rays as a result of SFPS is taken into account. It is shown that a weak (of the order of 10%) attenuation of the strong rays due to SFPS may lead to a significant change in SFPS efficiency compared to the efficiency when such attenuation is not taken into account. Possible causes of the discrepancy between the theory and experiments and also the effect of resonant photons on SFPS are discussed.

1. INTRODUCTION

We have previously reported observation of stimulated resonant parametric scattering of laser radiation in saturated vapors of atomic potassium[1] and rubidium[2]. When two beams propagate at a small angle θ between them through a cell with the saturated vapor, the weak beam was intensified and additional beams appeared at angles that were multiples of θ. This phenomenon was observed only when the frequency of the exciting radiation exceeded the frequency of the atomic transition, where the refractive index increased with increasing intensity of the incident beams, and the maximum effect was reached at a definite value of θ for the given intensity of the incident beams. These two factors have enables us to connect the observed phenomenon with the effect of stimulated four-photon parametric scattering (SFPS)[3-7]. However, the sharp asymmetry of the effect, experimentally observed from the short- and long-wave sides of the atomic-absorption lines, could not be explained quantitatively (and in some cases even qualitatively) within the framework of the existing SFPS theories[8]. These theories make us of the given-field approximation with respect to the strong beam, when the attenuation of the strong beam is neglected. The limits of applicability of such an approximation are far from obvious, since the intensities of the strong beam determine not only the parametric amplification coefficient, but also the condition for the phase synchronism of the parametric interaction of the four waves.

In the present communication we discuss in greater detail the conditions of the experiment and the experimental result obtained by us, and also the results of a theoretical analysis of SFPS, carried out with allowance for the attenuation of the strong beam. This analysis has enabled us to explain qualitatively (and in some cases also quantitatively) the sharp asymmetry of the SFPS when the latter is observed from the long- and short-wave sides of the absorption line. We show that an insignificant attenuation (on the order of 10%) of the strong ray can lead to a rather appreciable change (by a factor of several times) in the efficiency of the SFPS in comparison with its efficiency without allowance for such an attenuation. The results of the theory developed by us coincide in the limiting case of infinitesimally small attenuation of the strong beam with the results of the existing SFPS theories[3,7] developed in the given-field approximation.

2. EXPERIMENT

The experimental setup for the observation of SFPS is shown in Fig. 1. An organic-dye layer (ODL) was excited by radiation, focused with a cylindrical lens having $f_1 = 200$ mm, from a ruby laser 1 with passive Q switching with a KS-19 filter ($P = 50$ MW, $\Delta t = 25$ nsec). That part of the ruby-laser radiation which passed through the cell 2 with the dye solution in the resonator of the driving ODL was focused by a second cylindrical lens ($f_2 = 30$ mm) onto a cell with a solution of the same dye but with somewhat higher concentration. In the investigation of SFPS in potassium vapor (absorption lines of the principal doublet with λ_0 equal to 7665 and 7669 Å), we used a solution of the dye 1, 1′-diethyl-2, 2′-dicarbocyanine iodide in glycerine (λ_{gen} equal to 760–770 nm). In the case of observation of SFPS in rubidium vapor (absorption lines of principal doublets with λ_0 equal to 7800 and 7948 Å) we used a solution of the dye 1,3,3′, 1′,3′,3′-hexamethylinedotricarbocyanine iodide in alcohol (λ_{gen} equal to 790–800 or 775–785 nm). The second cell 3 served as the power amplifier for the ODL radiation. Such a scheme has made it possible to increase the power density of the radiation of the driving ODL by 20–30 times, and to decrease its divergence appreciably, since we amplified only that weakly-divergent part of the driving ODL radiation, which passed through a narrow amplification region formed by the lens f_2 in the amplifier cell. The amplifier operated in a high-saturation regime, thereby greatly increasing the stability of the setup and the reproducibility of the amplitude of the ODL emission pulses from flash to flash. To prevent the amplifier from lasing, the cell 3 was placed at the Brewster angle to the amplified beam of the driving ODL. The

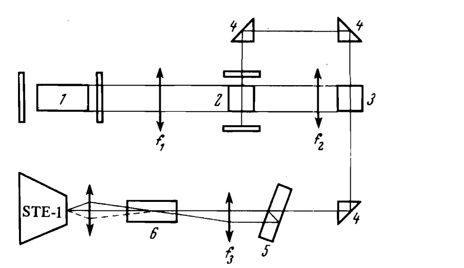

FIG. 1. Experimental setup for the observation of SFPS: 1–ruby laser, 2–driving organic-dye laser, 3–amplifier based on a dye solution; f_1, f_2, f_3–lenses; 4–prisms; 5–substrate with transparent dielectric coating; 6–cell with investigated vapor of alkali metal (K or Rb).

maximum intensity of the ODL beam was 10^8 W/cm^2 at a pulse duration $\Delta t = 25$ nsec.

The diaphragmed ODL beam, with 1 mm diameter and divergence $\sim 10^{-3}$ rad was then split, passing through a semitransparent mirror 5 inclined at a small angle. The two beams were brought together by a long-focus lens ($f = 550$ mm) in the cell with the investigated vapor of potassium or rubidium (length $l = 70$ mm), and then propagated in the cell with intensity ratio 1 : 50; the angle between them could be varied, by rotating the mirror, in the range $\theta = 10^{-3} - 10^{-2}$ rad. In the second variant of the scheme, the two beams were obtained with the aid of two diaphragms (each of 0.6 mm diameter, with a distance 1—4 mm between them) and were guided to the cell with the investigated vapor by a wedge placed in the path of one of the beams, or, as before, with a long-focus lens with $f = 550$ mm. The intensity of either beam could be varied with a neutral light filter, and their polarization could be varied with a system consisting of a quarter-wave plate and a polaroid. The distribution of the intensity over the angles in the spectrum of the radiation passing through the vapor was investigated with the aid of STÉ-1 spectrograph (dispersion 13 Å/mm).

The principal experimental results obtained in the observation of SFPS near each of the absorption D lines of K and Rb are the same. The threshold of reliable observation of SFPS corresponded to a scattering of approximately 2% of the incident-radiation energy in an angle of 10^{-3} rad.

SFPS Following Excitation by Two Beams with Intensity Ratio 1:50

1. At a pressure vapor $10^{-3} - 10^{-1}$ mm Hg and a strong-beam intensity $I_1 = 10^7 - 10^8$ W/cm^2 (width of the ODL generation spectrum ~ 100 Å), a distinct intensification of the weak beam is observed on the short-wave side of the absorption D lines of the investigated vapors at certain wavelengths that are close to the center of the corresponding absorption line, and an additional beam is produced at the same wavelength, in the plane of the incident beams, at an angle $\theta_{-3} = -\theta$ (Fig. 2b).

2. At a fixed vapor concentration and intensity I_1, there is an optimal angle θ_{opt} of maximum amplification. At θ_{opt}, the intensity of the additional beams always increased with increasing I_1. The maximum gain reached ~ 10, and the intensity I_{-3} of the additional beam was approximately equal to the intensity of the amplified weak beam I_{-1} (Fig. 2b). Attenuation of the strong beam I_1 is observed only at those wavelengths, at which the weak beam is amplified and the additional beam appears. The dependence of the efficiency of the SFPS on the angle θ between the beams has an asymmetrical character, namely, the SFPS efficiency decreases sharply at $\theta > \theta_{opt}$ and decreases more slowly at $\theta > \theta_{opt}$. The wavelength region where intensification of the weak beam is observed moves away from the absorption line with increasing vapor pressure or with decreasing θ, and also broadens when I_1 is increased.

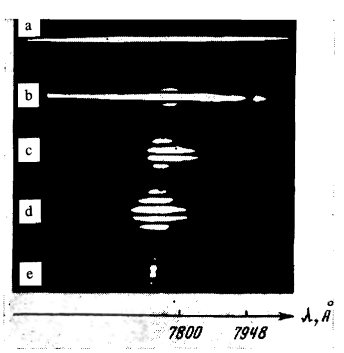

FIG. 2. Spectrogram of radiation passing through a cell with rubidium vapor: a—spectrum of incident radiation, the weaker beam has too low an intensity to be seen; b—incidence of two beams with intensity ratio 1:50; c—incidence of two beams of approximate equal intensity ($I_0 \approx 10^7$ W/cm^2); d—the same as in case c, but with $I_0 = 10^8$ W/cm^2; e—quasimonochromatic excitation with two beams of approximately equal intensity.

3. The SFPS effect is preserved also in the case of nonresonant excitation of the vapor by strong pulses of quasimonochromatic radiation from the ODL (spectrum width $\Delta\lambda = 1$ Å, $I_1 = 10^8$ W/cm^2, $\lambda_0 - \lambda = 6$ Å).

4. The maximum gain depends little on the vapor pressures and remains practically unchanged on going from linear to elliptic polarization of the ODL beam.

5. When the spectral components that resonate with the D line are eliminated from the spectrum of the incident beams, by placing a second cell with the vapor of the investigated metal in the path of the ODL beam prior to its splitting, the SFPS observed in the short-wave region is preserved or even increases somewhat.

SFPS Following Excitation with Two Beams of Comparable Intensity

1. When two beams of comparable intensity propagate in the cell with the investigated vapor, two beams are immediately produced at angles $\theta_{-3} = -\theta$ and $\theta_3 = 2\theta$ (Fig. 2c). The intensity of the additional beams always increased with increasing intensity of the incident beams. At the maximum employed intensities of the exciting beams ($\sim 10^8$ W/cm^2), the intensities of the transmitted and additional beams became approximately equal and new beams were produced at angles θ_n equal to -2θ, 3θ, etc. (Fig. 2d).

2. At not too large spectral intensities of the incident radiation ($\sim 10^7$ W/cm^2), elimination of the harmonics that resonate with the D lines from the incidence spectrum led to a vanishing of the additional lines. It must be emphasized that the intensity of the additional beams exceeded by at least one order of magnitude the intensity of the radiation absorbed in the D lines. This means that the onset of additional beams is not the result of the transfer of the energy of the radiation absorbed in the D lines. At large spectral excitation densities (for example, under conditions $\Delta\lambda = 1$ Å, $I_1 = 10^8$ W/cm^2, $\lambda_0 - \lambda = 6$ Å), the additional beams were produced also when harmonics resonant with the absorption D lines were eliminated from the spectrum of the incident radiation (Fig. 2e).

3. When the excitation is produced by two beams of approximately equal intensity, the SFPS effect is observed at lower excitation densities than in the case when the SFPS is excited by beams with an intensity ratio 1 : 50 (in this case the integral intensity of the exciting beams is the same).

4. The dependence of the SFPS efficiency on the angle θ between the beams does not have a clearly pronounced maximum as in the case of two beams that

differ strongly in intensity. The intensity of the additional beams changed negligibly at small angles θ and decreases sharply when the angle θ increases above a certain critical value ($\sim 5 \times 10^{-3}$ rad).

5. In all cases, there was no SFPS effect when the polarization planes of the incident beams I_1 and I_{-1} were mutually perpendicular.

3. THEORY

Under the conditions of our experiment, the SFPS was observed both with quasimonochromatic ODL radiation and with broad-spectrum radiation. Nonetheless, the interpretation of the results that are not connected with the influence of the resonant radiation at the frequency ω_0 of the atomic absorption line, we shall consider the SFPS of monochromatic radiation of frequency ω without a change in the frequency of the scattered radiation (degenerate SFPS). In addition to the difficulty entailed in the consideration of the more general problem of the SFPS of nonmonochromatic radiation, the basis for such an approach is the experimentally observed transfer of energy of the strong beam to a weak one at only one and the same wavelength (with accuracy to within ~Å). This experimental fact is in accord with the conclusion drawn by the authors of[7], that the threshold of the degenerate SFPS is lower than the threshold of the nondegenerate SFPS with different wavelengths of the incident and scattered beams. In addition, the theory of degenerate SFPS excited by two beams of greatly differing intensity, which we consider here, can be used to explain the results of the observation of the degenerate SFPS of ruby-laser emission in nitrobenzene[4] and in dye solutions[5].

We consider a nonlinear medium consisting of an ensemble of two-level atoms with transition frequency ω_0. In the case when a field $\mathbf{E}_\omega$ of frequency ω close to ω_0 acts monochromatically on such a medium, the polarization vector $\mathbf{P}$ is given by[9]

$$\mathbf{P} = \mathbf{P}_\omega e^{-i\omega t} = \frac{\alpha_\omega \mathbf{E}_\omega}{1 + a_\omega |\mathbf{E}_\omega|^2} e^{-i\omega t} = \chi_\omega \mathbf{E}_\omega e^{-i\omega t}, \quad (1)$$

$$\alpha_\omega = \frac{N|d|^2}{\hbar(\omega_0 - \omega - i\gamma_2)}, \quad a_\omega = \frac{4|d|^2\gamma_2}{\gamma_1[\gamma_2^2 + (\omega_0 - \omega)^2]\hbar^2}, \quad \chi_\omega = \frac{\alpha_\omega}{(1 + a_\omega|\mathbf{E}_\omega|^2)}.$$

Here α_ω is the linear polarizability of the medium, N is the concentration of the atoms, d is the dipole matrix element of the transition, a_ω is the saturation parameter, γ_1 and γ_2 are the velocities of the longitudinal and transverse relaxations. We assume that the condition $|\omega_0 - \omega| \gg \gamma_2$ is satisfied, wherein the nonlinear polarizability χ_ω is a real quantity, corresponding to neglecting the attenuation of the waves in the medium[1)].

The propagation and interaction of the waves in the considered medium will be described by a Maxwell wave equation for transverse waves with nonlinear polarization vector

$$\Delta \mathbf{E}_\omega + \frac{\omega^2}{c^2}\mathbf{E}_\omega = -\frac{4\pi\omega^2}{c^2}\mathbf{P}_\omega. \quad (2)$$

In accordance with the experiment, we start with the following formulation of the problem. Two waves $\mathbf{E}_1$ and $\mathbf{E}_{-1}$ with wave vectors $\mathbf{k}_1$ and $\mathbf{k}_{-1}$ are incident on the boundary of the medium $z' > 0$ (Fig. 3). The polarizations of the incident waves are assumed to be plane and directed on the boundary $z' = 0$ along the y' axis. This assumption enables us to consider, in place of the vector equation (2), a scalar equation[2)] for the projection of $\mathbf{E}_\omega$ on the y' axis. The boundary condition of the problem is formulated by using the fact that the discontinuity of the refractive index on the boundary of the medium be much smaller than unity, and the beams are almost normally incident. Under these conditions, neglecting reflection at the boundary, we assume the field at the boundary to be given and equal to the value of the field outside the medium.

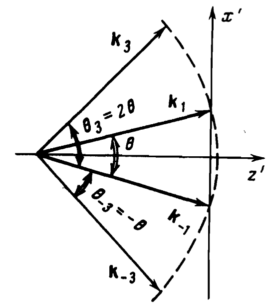

FIG. 3. Diagram of beam propagation in SFPS.

The next simplification is obtained by assuming that the incident radiation is incapable of saturating the absorption line, i.e., $a_\omega |\mathbf{E}|^2 < 1$. Expanding the nonlinear polarizability χ_ω in a series in the field intensity and confining ourselves to the term linear in the intensity, we rewrite (2) in the form

$$\left(\frac{\partial^2}{\partial z'^2} + \frac{\partial^2}{\partial x'^2} + \frac{\omega^2}{c^2}\right) E_\omega = -4\pi\alpha_\omega \frac{\omega^2}{c^2}(1 - a_\omega |E_\omega|^2) E_\omega. \quad (3)$$

Putting

$$E_\omega = \mathcal{E}'(x', z') \exp(ik_0 z'), \qquad k_0^2 = \frac{\omega^2}{c^2}(1 + 4\pi\alpha_\omega)$$

and neglecting the term $\partial^2\mathcal{E}/\partial z'^2$ in comparison with $k_0 \partial\mathcal{E}'/\partial z'$, we obtain the abbreviated equation

$$2ik_0 \frac{\partial \mathcal{E}'}{\partial z'} + \frac{\partial^2 \mathcal{E}'}{\partial x'^2} = 4\pi\alpha_\omega k_0^2 a_\omega \mathcal{E}' |\mathcal{E}'|^2. \quad (4)$$

Equation (4) takes the following form in terms of the dimensionless variables $x = x'k_0\theta$, $z = z'k_0\theta^2$, and $\mathcal{E} = \mathcal{E}'/\mathcal{E}_0$:

$$2i\frac{\partial \mathcal{E}}{\partial z} + \frac{\partial^2 \mathcal{E}}{\partial x^2} = \beta \mathcal{E} |\mathcal{E}|^2, \quad (5)$$

where $\mathcal{E}_0 = (|\mathcal{E}_1^0|^2 + |\mathcal{E}_{-1}^0|^2)^{1/2}$, $\beta = 4\pi a_\omega \mathcal{E}_0^2 \alpha_\omega/\theta^2$, $\mathcal{E}_1^0$ and $\mathcal{E}_{-1}^0$ are the amplitudes of the waves on the boundary of the medium. We note that the sign of β determines the value of α_ω. Therefore in the short-wave region $\omega > \omega_0$ we have $\beta < 0$. The boundary condition of the problem has the following form in the dimensionless variables:

$$\mathcal{E}(x, z = 0) = \mathcal{E}_1^0 e^{ix} + \mathcal{E}_{-1}^0 e^{-ix}. \quad (6)$$

The periodic boundary condition in x can be satisfied by a solution in the form

$$\mathcal{E}(x, z) = \sum_{n=-\infty}^{+\infty} \mathcal{E}_n'(z) e^{inx} \quad (7)$$

under the condition

$$\mathcal{E}_1'(z=0) = \mathcal{E}_1^0, \quad \mathcal{E}_{-1}'(z=0) = \mathcal{E}_{-1}^0, \quad \mathcal{E}_n' = 0 \quad \text{for } n \neq 1, -1. \quad (8)$$

The amplitude $\mathcal{E}_n'$ satisfy the system of equations

$$2i\frac{d}{dz}\mathcal{E}_n' - n^2\mathcal{E}_n' = 2\mathcal{E}_n'\beta \sum_{-\infty}^{\infty} |\mathcal{E}_k'|^2 - \beta\mathcal{E}_n'|\mathcal{E}_n'|^2 + \beta \sum_{n=m+k-l}'' \mathcal{E}_m'\mathcal{E}_k'\mathcal{E}_l'^{*}. \quad (9)$$

The primes at the summation sign denote here that m, $k \neq n$. The quantity $\sum_k |\mathcal{E}_k'|^2$ is an integral of the system (9), i.e., it does not depend on z; this expresses the energy conservation law, and therefore, by introducing the substitution

$$\mathscr{E}_n = \mathscr{E}_n' \exp\Big(-i\beta z \sum_k |\mathscr{E}_k|^2\Big),$$

we obtain

$$2i\frac{d}{dz}\mathscr{E}_n - n^2\mathscr{E}_n = -\beta\mathscr{E}_n|\mathscr{E}_n|^2 + \beta\sum_{n=m+k-l}'' \mathscr{E}_m\mathscr{E}_k\mathscr{E}_l^*. \qquad (10)$$

The first term on the right describes here the self-action of the wave, namely the nonlinear increment to the refractive index, while the second term describes the parametric interaction of the wave.

Equation (10) is the fundamental one in the research that follows. The summation condition $n = m + k - l$ connects the exciting waves $\mathscr{E}_1$ and $\mathscr{E}_{-1}$ only with the odd harmonics $\mathscr{E}_{-3}$, $\mathscr{E}_3$, $\mathscr{E}_{-5}$, $\mathscr{E}_5$, etc. so that the intensity of the even harmonic will henceforth be regarded as negligibly small.

SFPS Following Excitation by a Strong and a Weak Wave: $|\mathscr{E}_1^0| \gg |\mathscr{E}_1^0|$

In this case we see from (10) that $|\mathscr{E}_{-3}|$ is small in comparison with $|\mathscr{E}_1|$, $|\mathscr{E}_{-1}|$, and $|\mathscr{E}_3|$ until the amplitudes $|\mathscr{E}_1|$, $|\mathscr{E}_{-1}|$, and $|\mathscr{E}_3|$ become equalized. Excitation of the wave $\mathscr{E}_{-3}$ is due to the interaction terms of the form $\mathscr{E}_{-1}^2\mathscr{E}_1^*$ or $\mathscr{E}_1\mathscr{E}_{-1}\mathscr{E}_3^*$, whereas the amplitudes of the waves $\mathscr{E}_3$ and $\mathscr{E}_{-1}$ vary as a result of the interaction of the type $\mathscr{E}_1^2\mathscr{E}_{-1}^*$ and $\mathscr{E}_1^2\mathscr{E}_3^*$. We confine ourselves therefore to the case when the intensities of the waves $\mathscr{E}_{-1}$ and $\mathscr{E}_1$ are not close to each other. We note that the wave $\mathscr{E}_{-3}$ was not observed in the experiment, but the intensities of the waves $\mathscr{E}_{-1}$ and $\mathscr{E}_3$ constitute an appreciable fraction of the intensity of the wave $\mathscr{E}_1^0$ (up to 20%).

The system of equations for the waves $\mathscr{E}_1$, $\mathscr{E}_{-1}$, and $\mathscr{E}_3$ is given by

$$\begin{aligned} 2i\frac{d}{dz}\mathscr{E}_1 - \mathscr{E}_1 &= -\beta\mathscr{E}_1|\mathscr{E}_1|^2 + 2\beta\mathscr{E}_3\mathscr{E}_{-1}\mathscr{E}_1^*, \\ 2i\frac{d}{dz}\mathscr{E}_{-1} - \mathscr{E}_{-1} &= -\beta\mathscr{E}_{-1}|\mathscr{E}_{-1}|^2 + \beta\mathscr{E}_3^*\mathscr{E}_1^2, \\ 2i\frac{d}{dz}\mathscr{E}_3 - 9\mathscr{E}_3 &= -\beta\mathscr{E}_3|\mathscr{E}_3|^2 + \beta\mathscr{E}_1^2\mathscr{E}_{-1}^*. \end{aligned} \qquad (11)$$

The system of equations for $\mathscr{E}_1^*$, $\mathscr{E}_{-1}^*$, and $\mathscr{E}_3^*$ has not been written out, since it is obtained from the system (11) by the conjugation operation. We shall now construct an exact solution of the system (11).

It is easy to verify that the system (11) has two integrals

$$\begin{aligned} |\mathscr{E}_1|^2 + |\mathscr{E}_{-1}|^2 + |\mathscr{E}_3|^2 &= 1, \\ |\mathscr{E}_{-1}|^2 - |\mathscr{E}_3|^2 &= \delta, \end{aligned} \qquad (12)$$

where $\delta = |\mathscr{E}_{-1}^0| \ll 1$. It will be convenient to change over to a new variable

$$\vartheta = \mathscr{E}_1 \exp\Big\{-\frac{i}{2}\int_0^z (\beta|\mathscr{E}_1|^2 - 1)\,dz\Big\}. \qquad (13)$$

The inverse transformation takes the form

$$\mathscr{E}_1 = \vartheta \exp\Big\{\frac{i}{2}\int_0^z (\beta|\vartheta|^2 - 1)\,dz\Big\}. \qquad (14)$$

By virtue of the first equation of the system (11), the quantity ϑ satisfies the equation

$$i\frac{d}{dz}\vartheta = \beta\mathscr{E}_3\mathscr{E}_{-1}\vartheta^* \exp\Big\{-i\int_0^z (\beta|\vartheta|^2 - 1)\,dz\Big\}. \qquad (15)$$

The last two equations of the system (11) enable us to write down an equation for the quantity $\mathscr{E}_{-1}\mathscr{E}_3$, which enters in (15):

$$2i\frac{d}{dz}(\mathscr{E}_{-1}\mathscr{E}_3) - 10\mathscr{E}_{-1}\mathscr{E}_3 = -\beta(1-|\vartheta|^2)\mathscr{E}_{-1}\mathscr{E}_3 + \beta(1-|\vartheta|^2)\vartheta^2 \times \exp\Big\{i\int_0^z (\beta|\vartheta|^2 - 1)\,dz\Big\}. \qquad (16)$$

Differentiating (15) with respect to z and eliminating the explicit dependence on z with the aid of (15) and its complex conjugate, and eliminating the dependence on $\mathscr{E}_{-1}\mathscr{E}_3$ with the aid of (16) and the relation

$$|\mathscr{E}_{-1}\mathscr{E}_3|^2 = \tfrac{1}{4}[(1-|\vartheta|^2)^2 - \delta^2],$$

which follows from (12), we obtain

$$\frac{d^2}{dz^2}\vartheta + i\frac{d\vartheta}{dz}\Big(4 + \frac{3}{2}\beta|\vartheta|^2 - \frac{\beta}{2}\Big) - \frac{\beta^2}{4}(1 - 4|\vartheta|^2 + 3|\vartheta|^4 - \delta^2)\vartheta = 0. \qquad (17)$$

Equation (17) together with its complex conjugate for the quantity ϑ^* and together with (14) describes the dynamics of the wave $\mathscr{E}_1$. It is easy to verify that the two equations for ϑ and ϑ^* can be written in the form of a single equation for the real vector quantity $\mathbf{r} = \mathbf{i}\,\mathrm{Re}\,\vartheta + \mathbf{j}\,\mathrm{Im}\,\vartheta$:

$$\frac{d^2\mathbf{r}}{dz^2} = \Big[\frac{d\mathbf{r}}{dz} \times \mathbf{H}\Big] - \frac{\partial U}{\partial \mathbf{r}}. \qquad (18)$$

Here

$$\mathbf{H} = \mathbf{k}\Big(4 + \frac{3}{2}\beta r^2 - \frac{\beta}{2}\Big) = \mathbf{k}H, \qquad (19)$$

$$-\frac{\partial U}{\partial \mathbf{r}} = (1 - 4r^2 + 3r^4 - \delta^2)\frac{\beta^2}{4}\mathbf{r}, \qquad (20)$$

i, j, and k are three mutually perpendicular unit vector and $r^2 = \mathbf{r}^2$. Equation (18) is analogous to the equation describing the dynamics of the charged particle in an electric field $-\partial U/\partial \mathbf{r}$ and a magnetic field H. We shall use this analogy later on. In particular, the square of the "distance of the point from the axis," or the quantity r^2, is simply the intensity of the wave $\mathscr{E}_1$.

The conservative character of the "force" $-\partial U/\partial \mathbf{r}$ and the axial symmetry of the field H make it possible to write down two integrals of motion: the energy conservation law

$$\frac{1}{2}\Big(\frac{d\mathbf{r}}{dz}\Big)^2 + U = \mathrm{const} = C_1 \qquad (21)$$

and the law of conservation of the total angular momentum

$$\Big[\mathbf{r} \times \frac{d\mathbf{r}}{dz}\Big] + W\mathbf{k} = \mathrm{const} = \mathbf{C}_2. \qquad (22)$$

Here the potential W of the field H is determined by the relation

$$\frac{\partial}{\partial z}W = rH. \qquad (23)$$

The values of the constants in (21) and (22) are determined from the boundary condition $dr/dz(z = 0) = 0$ (see (8) and (15)):

$$C_1 = U(r|_{z=0}) = U(r_0) = U_0, \qquad \mathbf{C}_2 = W(r_0)\mathbf{k} = W_0\mathbf{k}. \qquad (24)$$

Expressing the total "velocity" $d\mathbf{r}/dz$ in terms of the radial velocity dr/dz from (22) and substituting $d\mathbf{r}/dz$ in (21), we obtain an equation describing the dynamics of the radial motion:

$$\frac{1}{2}\Big(\frac{dr}{dz}\Big)^2 + \frac{(W - W_0)^2}{2r^2} + U - U_0 = 0. \qquad (25)$$

It is convenient further to introduce the quantity

$\rho = r^2 = |\vartheta|^2 = |\mathscr{E}_1|^2$, which is equal to the energy of the wave $\mathscr{E}_1$. By virtue of the integrals (12), the quantity ρ determines simultaneously the energies of the wave $\mathscr{E}_3$ and $\mathscr{E}_{-1}$:

$$|\mathscr{E}_3|^2 = (1-\rho-\delta)/2, \quad |\mathscr{E}_{-1}|^2 = (1-\rho+\delta)/2. \tag{26}$$

Equation (25) for ρ with allowance for (19), (20), and (23) takes the form

$$\left(\frac{d\rho}{dz}\right)^2 + \left[\int\limits_{\rho_0}^{\rho}\left(4+\frac{3}{2}\beta\rho-\frac{\beta}{2}\right)d\rho\right]^2 - \rho\beta^2\int\limits_{\rho_0}^{\rho}(1-4\rho+3\rho^2-\delta^2)\,d\rho = 0. \tag{27}$$

Here $\rho_0 = r_0^2 = |\mathscr{E}_1^0|^2 = 1 - \delta$.

Thus, the change of the energy of the wave $\mathscr{E}_1$ is simulated by the equation of motion of the particle with zero energy in a one-dimensional potential well:

$$(d\rho/dz)^2 + U_{eff} = 0, \tag{28}$$

where the potential U_{eff} is given by

$$U_{eff} = (\rho-\rho_0)^2\{[4 - {}^1\!/_2\beta + {}^3\!/_4\beta(\rho+\rho_0)]^2 - \beta^2\rho^2\} + 2\beta^2\rho^2\delta(\rho-\rho_0). \tag{29}$$

The point begins its motion from the position ρ_0 with zero initial velocity, reaches the turning point, and begins its return motion. Accordingly, the energy of the wave $\mathscr{E}_1$ decreases to a certain value and then returns to the initial value, etc. Thus, the turning point determines the minimum energy of the wave $\mathscr{E}_1$ or the maximum energies of the waves E_{-1} and E_3. The position of the turning point is determined by the value ρ_S ($0 < \rho_S < \rho_0$) of the roots of the equation[3)] $U_{eff}(\rho_S) = 0$ closest to ρ_0.

We shall not investigate here in detail the motion of $\rho(z)$, although the form of the function $U_{eff}(\rho)$ makes it possible to express $\rho(z)$ in terms of an elliptic integral, and will determine the position of the turning point, given by the equation

$$(\rho_s-\rho_0)\left(4+\frac{\beta}{4}-\frac{\beta}{4}\rho_s-\frac{3\beta}{4}\delta\right)\left(4+\frac{\beta}{4}+\frac{7}{4}\beta\rho_s-\frac{3\beta}{4}\delta\right)+2\beta^2\delta\rho_s^2=0. \tag{30}$$

It can be solved by successive approximations with respect to the small parameter δ. Figure 4 shows the dependence of the maximum energy $\rho_3 = (\rho_0 - \rho_S)/2$ on β at $\delta = 0.02$. At $\rho_3|\beta| \ll 16$ we can represent ρ_S in the form

$$\rho_s = \frac{8+4\beta}{7\beta}\left[1 \pm \left(1-\frac{7\beta^2\delta}{8(2+\beta)^2}\right)^{1/2}\right] \tag{31}$$

with a plus sign in front of the expression in the round brackets for $\beta < -2$ and with a minus sign for $\beta > -2$. This relation shows the substantial difference between the SFPS efficiencies in the short- and long-wave regions.

An exact estimate of the period of the intensity oscillations of the scattered waves is a rather cumbersome problem. We confine ourselves to a rough estimate of l_n, by approximating the exact potential $U_{eff}(\rho)$ by a parabolic one in the region where the motion is allowed. The estimate of l_n for $|\beta| = 2$, obtained in this manner, yields $l_n = 1$–2 cm.

SFPS For Excitation with Two Waves of Equal Intensity

In this case, the boundary condition $\mathscr{E}(z=0) = \mathscr{E}_{-1}^0 e^{-ix} + \mathscr{E}_1^0 e^{ix}$, with a suitably chosen origin for x, can be expressed in the form

$$\mathscr{E}(z=0) = \mathscr{E}^0 \cos x, \tag{32}$$

where $|E^0| = |E_{-1}^0| = |E_1^0|$. Since the function $\mathscr{E} = \mathscr{E}^0$

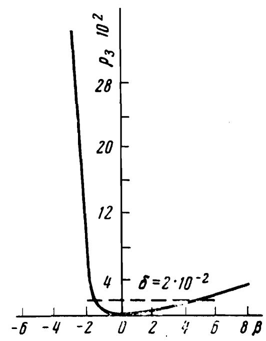

FIG. 4

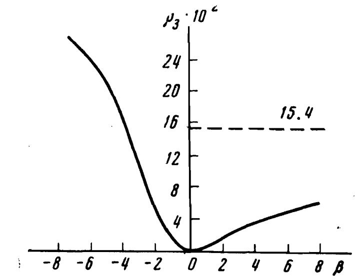

FIG. 5

FIG. 4. Dependence of the maximum wave energy ρ_3 on β for SFPS excitation by two beams with intensity ratio 1:50.

FIG. 5. Dependence of the maximum wave energy ρ_3 on β for SFPS excitation by beams of equal intensity

cos x is even and Eq. (5) is invariant to the replacement of x by −x, we can seek the solution in the form of an even function of x, i.e., it is correct to put in the expansion (7)

$$\mathscr{E}_n(z) = \mathscr{E}_{-n}(z). \tag{33}$$

We confine our analysis to the case of the four waves $\mathscr{E}_{\pm1}$ and $\mathscr{E}_{\pm3}$. As before, this limitation is valid so long as the intensities of the waves $\mathscr{E}_{\pm3}$ and $\mathscr{E}_{\pm1}$ are not close. Taking (33) into account, the equation for $\mathscr{E}_1$ and $\mathscr{E}_3$ take the form

$$2i\frac{d}{dz}\mathscr{E}_1 - \mathscr{E}_1 = -\beta\mathscr{E}_1|\mathscr{E}_1|^2 + \beta\mathscr{E}_1^2\mathscr{E}_3^* + 2\beta\mathscr{E}_3|\mathscr{E}_1|^2 + \beta^2\mathscr{E}_3^2\mathscr{E}_1^*,$$
$$2i\frac{d}{dz}\mathscr{E}_3 - 9\mathscr{E}_3 = -\beta\mathscr{E}_3|\mathscr{E}_3|^2 + \beta\mathscr{E}_1|\mathscr{E}_1|^2 + 2\beta\mathscr{E}_3^*\mathscr{E}_1^2. \tag{34}$$

The corresponding equations for $\mathscr{E}_1^*$ and $\mathscr{E}_3^*$ are obtained by complex conjugation of the system (34). The latter has an obvious integral $|\mathscr{E}_1|^2 + |\mathscr{E}_3|^2 = \rho_1 + \rho_3 = 0.5$. We are interested in the intensities ρ_1 and ρ_3 of the waves $\mathscr{E}_1$ and $\mathscr{E}_3$, respectively. The equations describing the change of ρ_1 and of the associated quantity $\rho_{13} = \rho_{31}^* = \mathscr{E}_1\mathscr{E}_3^*$ are obtained from (34) and from the system complex-conjugate to it, and take the form

$$-2i\frac{d}{dz}\rho_1 = \beta\rho_1(\rho_{13}-\rho_{31}) + 2\beta(\rho_{13}^2-\rho_{31}^2),$$
$$2i\frac{d}{dz}\rho_{13} + 8\rho_{13} = \beta\rho_{13}^2 + \beta\rho_{13}(\rho_3-\rho_1) + 2\beta\rho_{31}(\rho_3-\rho_1) + 2\beta\rho_3\rho_1 - \beta\rho_1^2, \tag{35}$$
$$2i\frac{d}{dz}\rho_{31} - 8\rho_{31} = -\beta\rho_{31}^2 - \beta\rho_{31}(\rho_3-\rho_1) - 2\beta\rho_{13}(\rho_3-\rho_1) - 2\beta\rho_3\rho_1 + \beta\rho_1^2.$$

These equations are not independent, in view of the relation

$$\rho_{13}\rho_{31} = \rho_1\rho_3 = \rho_3({}^1\!/_2 - \rho_3), \tag{36}$$

but are compatible. The first equation is the consequence of the two other when the condition (36) is satisfied. Adding the second and third equations and eliminating the quantities $\rho_{13}^2 - \rho_{31}^2$ and $\rho_{13} - \rho_{31}$ with the aid of the first equation, we obtain one more integral of the system

$$\left(\rho_{13}+\rho_{31}+\frac{\rho_1}{2}\right)^2 + \frac{1}{\beta}\left(\frac{3}{4}\beta\rho_1^2 - 8\rho_1 - \frac{\beta}{2}\rho_1\right) = \text{const} = -\frac{4}{\beta}. \tag{37}$$

After squaring the right and left sides of the first equation of the system (35) and eliminating ρ_{13} and ρ_{31} with the aid of (36) and (37) we obtain

$$(d\rho_1/dz)^2 + U_{eff} = 0, \tag{38}$$

where

$$U_{eff} = -\beta\left(8\rho_1 - 4 + \frac{\beta}{2}\rho_1 - \frac{3}{4}\beta\rho_1^2\right)\left[4\rho_1\left(\frac{1}{2} - \rho_1\right) - \left(-\frac{\rho_1}{2} + \left\{\frac{1}{\beta}\left(8\rho_1 - 4 + \frac{\beta\rho_1}{2} - \frac{3}{4}\beta\rho_1^2\right)\right\}^{1/2}\right)^2\right]. \quad (39)$$

The position of the turning point ρ_3^S is determined by the following inverse relation:

$$|\beta| = \frac{8\rho_3^{1/2}}{(1/2 - \rho_3)\,[2(1/2 - \rho_3)^{1/2} \pm 3\rho_3^{1/2}]}, \quad (40)$$

in which the plus sign is for $\beta < 0$ and the minus sign for $\beta > 0$. From the $\rho_3^S(\beta)$ plot shown in Fig. 5 we see the difference between the SFPS in the short-wave ($\beta < 0$) and the long-wave ($\beta > 0$) regions; this difference, however, is smaller in the case of SFPS excited by beams of greatly differing intensity.

The intensity ratio in the short- and long-wave regions, at equal intensities of the strong beams, ranged from 1 to 6. At the maximum strong-beam intensities used in the experiments we got the value $\rho = 3-5$ at which the theory predicts a noticeable intensity ($\rho_3 = (2-4) \times 10^{-2}$) of the $\mathscr{E}_3$ wave and the long-wave region $\beta > 0$. An estimate of the length of the spatial period l_n yields $l_n = 3-6$ cm.

4. DISCUSSION OF RESULTS

Our problem was limited to a qualitative comparison of our experimental data with the developed theory of degenerate SFPS. A rigorous quantitative comparison is made difficult by the insufficient accuracy of the available experimental data. In addition, the developed theory pertains to degenerate stationary SFPS of plane monochromatic waves, whereas in our experiments we used nonmonochromatic pulsed radiation (the pulse duration was close to the lifetime of the excited $5P_{3/2,1/2}$ states of Rb atoms) with finite dimensions of the beams and with a divergence angle smaller by a factor of only 3–10 than the angle between the incident beams.

In the region $\omega > \omega_0$, the phenomena occurring in the excitation of SFPS by two beams with comparable intensities (noted in subsections 1, 3, and 5 of Sec. 2), or with a ratio 1 : 50 (subsections 1–4) are described satisfactorily, at any rate qualitatively, by the theory of degenerate SFPS in the given-field approximation[2,7]

The greatest difficulties are encountered in the interpretation of the observed sharp asymmetry of the SFPS on the short- and long-wave sides of the atomic-absorption lines. The observed difference between the intensity of the weak scattered waves in these regions at a beam intensity ratio 1 : 50 exceeds by at least one order of magnitude the value predicted by the theory of the degenerate SFPS in the approximation of the given field with respect to the strong beam[2,7]. Allowance for the attenuation of the strong beams makes it possible to explain satisfactorily the observed asymmetry. In particular, it follows from Fig. 4 that at a "threshold" intensity $|\beta| = 2$ in the short-wave region, the maximum attainable intensity of the scattered additional beam is 11% of the intensity of the incident strong beam, and in the long-wave region it is 0.5% (less than the threshold of observation of the SFPS in our experiments, which is ~2%).

The SFPS theory developed here for exciting beams with substantially differing intensities explains also the lower parametric amplification of a ruby-laser emission in nitrobenzene, obtained in[4], in comparison with that obtained from the theory in the approximation with a given strong-beam field.

The SFPS theory in the given-field approximation for two beams of equal intensity leads to only an insignificant asymmetry of the effect in the short- and long-wave regions of the atomic-absorption lines, whereas in experiment the effect is observed only in the short-wave region. The theory developed here describes the difference between the intensities of the scattered waves in the short- and long-wave regions, which agrees qualitatively with experiment, but the quantitative correspondence is unsatisfactory. One of the reasons for this, in our opinion, is that the theory was developed for plane incident waves, whereas in the experiments the beams had finite dimensions with a divergence commensurate with the angle between them. Our estimates for diverging beams show that finite dimensions of the beams decrease the SFPS efficiency (approximately twice as strongly in the region $\beta > 0$ than at $\beta < 0$). In addition, the finite divergence of the beams leads to a smoothing of the spatial pulsations of the scattered-wave intensity.

The role of the resonant photons in the SFPS process cannot be investigated within the framework of the theory of degenerate SFPS of monochromatic waves, and the more complicated processes of scattering of nonmonochromatic radiation must be brought into play. The susceptibility of the resonant system in the case of a nonmonochromatic strong radiation field was considered recently a number of times (see, for example,[9,10]). The character of the susceptibility is determined by the statistical properties of the radiation. We assume that the nonmonochromatic radiation is stationary Gaussian noise. It can be shown that if the radiation-spectrum width $\Gamma \gg \gamma_1, \gamma_2$ and $\gamma_2 \gg \gamma_1$, then the fluctuations of the population of the excited state of the two-level system are small in comparison with the average population. The susceptibility of the two-level system can then be written in the form[9]

$$\chi_\omega = \frac{\alpha_\omega}{1 + d^2 I_0/\gamma_1 \hbar^2}, \quad (41)$$

where I_0 is the spectral density of the irradiation at the frequency $\omega = \omega_0$. Formula (41) shows that both the change in the synchronism condition and the SFPS gain depend on the radiation density at the frequency of the absorption line. A detailed theory of SFPS for nonmonochromatic action can be constructed in analogy with that developed above, but the need for taking absorption into account, which leads to a change of I_0 along the z' axis, introduces significant difficulties into the theory.

---

[1]Strictly speaking, the condition $|\omega_0 - \omega| \gg \gamma_2$ is insufficient to be able to neglect the influence of the wave attenuation in the medium on the SFPS. In order for the attenuation to have little influence on the SFPS it is necessary that the attenuation length l_ω be much larger than the characteristic length l_n of the nonlinear variation of the field as a result of the SFPS. Under the conditions of our experiment, at $|\omega_0 - \omega| \approx 10$ cm^{-1} and $l \approx 10-100$ cm, we have $l_n \approx 1-10$ cm.

[2]In the actual experiment the vector $\mathbf{E}$ was in the $z'0x'$ plane, but when the vectors of the incident waves were almost parallel (the angle between them was $\theta < 10^{-3}$ rad) the efficiency of the SFPS was practically independent of the direction of $\mathbf{E}_1$ or $\mathbf{E}_{-1}$. Of course, when the angle between the vectors of the incident waves was relatively large, the

efficiency of the SFPS vanished completely when the vectors E_1 and E_{-1} were mutually perpendicular.

3)The initial shift of the turning point occurs in the direction of $\rho < \rho_0$, since $\partial U_{eff}(\rho_0)/\partial\rho > 0$ in accordance with the physical meaning of the problem.

1. A. M. Bonch-Bruevich, V. A. Khodovoĭ, and V. V. Khromov, ZhETF Pis. Red. 11, 431 (1970) [JETP Lett. 11, 290 (1970)].
2. A. M. Bonch-Bruevich, N. N. Kostin, S. G. Przhibel' skiĭ, V. A. Khodovoĭ, V. V. Khromov, and N. A. Chigir', in: Nelineĭnye protsessy v optike (Nonlinear Processes in Optics), Proc. of Second Vavilov Conf. on Nonlinear Optics, 22–25 June 1971, Novosibirsk, No. 2, 1972.
3. R. Y. Chiao, P. L. Kelly, and E. Garmire, Phys. Rev. Lett., 17, 1158 (1966).
4. R. L. Carman, P. Y. Chiao, and P. L. Kelly, Phys. Rev. Lett., 17, 1281 (1966).
5. M. E. Mack, Appl. Phys. Lett., 12, 329 (1968).
6. Yu. M. Kirin, S. G. Rautian, A. E. Semenov, and B. M. Chernoborod, ZhETF Pis. Red. 11, 340 (1970) [JETP Lett. 11, 226 (1970)].
7. P. A. Apanasevich and A. A. Afanas'ev, Preprint, Physics Inst. Belorussian Acad. Sci., Minsk, 1972.
8. V. V. Khromov, Candidate's dissertation, Leningrad, 1972.
9. P. A. Apanasevich, Zh. Prikl. Spektrosk. 12, 231 (1970).
10. Yu. S. Oseledchik and Yu. N. Galutva, ibid. 17, 430 (1972).

Translated by J. G. Adashko
7